

Tennessee State University

Digital Scholarship @ Tennessee State University

Information Systems and Engineering
Management Research Publications

Center of Excellence in Information Systems
and Engineering Management

10-17-2019

HD 126516: A Triple System Containing a Short-period Eclipsing Binary

Francis C. Fekel
Tennessee State University

Gregory W. Henry
Tennessee State University

James R. Sowell
Georgia Institute of Technology

Follow this and additional works at: <https://digitalscholarship.tnstate.edu/coe-research>



Part of the [Stars, Interstellar Medium and the Galaxy Commons](#)

Recommended Citation

Francis C. Fekel et al 2019 AJ 158 189

This Article is brought to you for free and open access by the Center of Excellence in Information Systems and Engineering Management at Digital Scholarship @ Tennessee State University. It has been accepted for inclusion in Information Systems and Engineering Management Research Publications by an authorized administrator of Digital Scholarship @ Tennessee State University. For more information, please contact XGE@Tnstate.edu.



HD 126516: A Triple System Containing a Short-period Eclipsing Binary

Francis C. Fekel^{1,3} , Gregory W. Henry¹ , and James R. Sowell²

¹ Center of Excellence in Information Systems, Tennessee State University, 3500 John A. Merritt Boulevard, Box 9501, Nashville, TN 37209, USA
fekel@evans.tsuniv.edu, gregory.w.henry@gmail.com

² School of Physics, Georgia Institute of Technology, Atlanta, GA 30332, USA; jim.sowell@physics.gatech.edu
Received 2019 April 18; revised 2019 August 13; accepted 2019 August 16; published 2019 October 17

Abstract

From numerous radial velocities as well as Johnson *B* and *V* differential photoelectric photometry, we have determined the orbital elements and other properties of the single-lined triple system HD 126516. This system consists of a narrow-lined F5 V star and an unseen M dwarf companion in a 2.1241 day circular orbit. The small, low-mass secondary produces detectable eclipses of the primary, and that pair has been given the variable star name V349 Vir. Variations of the center-of-mass velocity of this short-period system have an orbital period of 702.7 days or 1.92 yr and an eccentricity of 0.36. The third star is likely a K or M dwarf. From an analysis of our photometry, we conclude that the primary of HD 126516 is not a γ Dor variable. Comparison with evolutionary tracks indicates that the primary is slightly metal-poor and has an age of 2.5 Gyr. The projected rotational velocity of the primary is very low, just 4 km s^{-1} , which is 10 times less than its synchronous rotational velocity. Thus, either that component's rotation is extremely non-synchronous or the inclinations of the rotational and orbital axes are very different, and so the primary has a very large spin-orbit misalignment. Because of the moderate age of the system and the fact that its orbit is already circularized, neither situation is expected theoretically.

Key words: eclipsing binary stars – spectroscopic binary stars – fundamental parameters of stars

Supporting material: machine-readable tables

1. Introduction

HD 126516 = HIP 70566 = NSV 20106 = V349 Vir ($\alpha = 14^{\text{h}}26^{\text{m}}03^{\text{s}}.09$, $\delta = -0^{\circ}41'30''.3$ (2000)) became an object of interest when Handler (1999) included it in his examination of the *Hipparcos* photometry (Perryman & ESA 1997) of about 450 stars. The goal of that search was to identify likely γ Dor pulsators. Those variables have late-A to early-F spectral classes, and so their instability strip overlaps that of the δ Sct variables in the Hertzsprung–Russell (H–R) diagram. Fortunately, the γ Dor stars have longer pulsation periods, 0.3–3 days (Kaye et al. 1999), than those of the δ Sct stars. While Handler (1999) identified 46 stars as prime γ Dor candidates, he found HD 126516 to have a weak signal with a single period of 0.493 days and, as a result, placed it in a list of possible but less likely γ Dor variables.

Fekel et al. (2003) made follow-up spectroscopic observations of over 30 γ Dor candidates identified by Handler (1999) and acquired four spectra of HD 126516. From those observations they found a radial velocity range of 72 km s^{-1} and identified it as a single-lined spectroscopic binary.

Otero & Wils (2005) analyzed the *Hipparcos* (Perryman & ESA 1997) and ASAS-3 (Pojmanski 2002) photometry of HD 126516, determined that it eclipses with a period of 2.12408 days, and classified it as an eclipsing binary of the Algol type. Their light curve shows just the primary eclipse which has a depth of only ~ 0.05 mag in *V*. As a result of this discovery, Kazarovets et al. (2008) assigned it the variable star name V349 Vir.

As part of another spectroscopic survey that included both confirmed and candidate γ Dor pulsators, De Cat et al. (2006)

obtained nine observations of HD 126516. Their spectra showed no line profile variations, so there was no indication of pulsation. They combined the velocities of Fekel et al. (2003) with their own and determined preliminary orbital elements including a period of 2.1245 days. Along with 11 other confirmed and possible γ Dor stars, Bruntt et al. (2008) determined the effective temperature and metal abundances of HD 126516. Kahraman Alicavus et al. (2016) also found its effective temperature and metal abundance.

Fekel et al. (2003) classified HD 126516 as F5 IV–V in excellent agreement with the F5 V spectral type of Kahraman Alicavus et al. (2016) and in reasonable accord with the F3 V classification of Moore & Paddock (1950). The star is very narrow lined with a $v \sin i$ value of $4\text{--}5 \text{ km s}^{-1}$ (Fekel et al. 2003; De Cat et al. 2006; Kahraman Alicavus et al. 2016).

After Fekel et al. (2003) found significant radial velocity variations, we acquired additional velocities to determine an orbit and found systematic residuals indicating a third component in the system. With the discovery by Otero & Wils (2005) that the short-period components eclipse, we also placed the system on our photometric observing program. The very narrow lines of the primary of the short-period eclipsing binary suggest a very large spin-orbit misalignment.

Our analysis of the spectroscopic and photometric data provides the basic properties of the triple system. Such a knowledge of the orbits of multiple systems is needed for an understanding of their origin (Tokovinin 2008). In addition, our results are a starting point for the understanding of the apparent spin-orbit misalignment of the primary component.

The spectroscopic observations and their reduction are discussed in Section 2. In Section 3 we determine the short- and long-period spectroscopic orbits from the radial velocities. The photometric data and reductions are reported in Section 4. In Section 5 we obtain a combined light and radial velocity

³ Visiting Astronomer, Kitt Peak National Observatory, National Optical Astronomy Observatory, operated by the Association of Universities for Research in Astronomy, Inc. under cooperative agreement with the National Science Foundation.

Table 1
Telescope and Detector Combinations

Telescope	CCD Detector	No. of Spectra	Years Observed	Central Wavelength (Å)	Wavelength Range (Å)	Resolving Power	Typical S/N
KPNO coudé feed	TI	42	2000–2010	6430	84	30000	100
KPNO coudé feed	STA2	6	2011	6430	336	30000	100
Fairborn 2 m AST	SITe ST-002A	85	2004–2011	6010	2180	35000	60
Fairborn 2 m AST	Fairchild 486	101	2011–2018	6200	4800	25000/15000	125

solution of the short-period system. The properties of the triple system and its components are discussed in Section 6.

2. Spectroscopic Observations and Reductions

We began our observations of HD 126516 at the Kitt Peak National Observatory (KPNO) in 2000 July and continued through 2011 June. During that time, we acquired 48 spectra with the coudé feed telescope, coudé spectrograph, and two different detectors. From 2000 through 2010 we used a Texas Instruments (TI) CCD and centered the spectra in the red at 6430 Å. The wavelength range is just 84 Å, and the spectra have a resolution of 0.21 Å or a resolving power of about 30,000. After the TI CCD was retired, we obtained spectra in 2011 with a CCD made by Semiconductor Technology Associates, designated STA2. That CCD consists of a 2600×4000 array of $12 \mu\text{m}$ pixels producing a wavelength range of 336 Å for spectra centered at 6430 Å. While the resolution of the latter spectra was set to be the same as that of our TI CCD spectra, the resolution worsens toward both ends of the STA2 spectra. The KPNO spectra have typical signal-to-noise ratios (S/N) of about 100.

For the KPNO spectra, we used the various spectrum reduction programs in IRAF (Tody 1986, 1993) for bias subtraction, flat fielding, and continuum rectification. Spectra of a thorium-argon hollow-cathode lamp were taken every 1–2 hr to enable wavelength calibration. IAU radial velocity standards were acquired throughout the night to provide spectra of stars with known velocities for cross-correlation with our spectra of HD 126516.

We obtained an additional 186 useful observations of HD 126516 at the Fairborn Observatory in southeastern Arizona from 2004 December through 2018 January with the Tennessee State University 2 m Automatic Spectroscopic Telescope (AST), fiber-fed echelle spectrograph, and a CCD detector (Eaton & Williamson 2004). From 2004 through 2011 we used a 2048×4096 SITe ST-002A CCD with $15 \mu\text{m}$ pixels.

Eaton & Williamson (2007) explained the reduction and wavelength calibration of the raw Fairborn Observatory spectra. Those SITe echelle spectrograms have 21 orders that cover the wavelength range 4920–7100 Å. The observations have an average resolution of 0.17 Å, which corresponds to a resolving power of 35,000 at 6000 Å. Although a typical S/N value for these spectra is 60, the dewar was unable to maintain constant temperature, and the significant temperature variations resulted in the reduction of S/Ns for some of the spectra.

During the summer of 2011, the SITe CCD and its dewar were replaced with a Fairchild 486 CCD that has a 4096×4096 array of $15 \mu\text{m}$ pixels and a new dewar (Fekel et al. 2013b). The expanded wavelength coverage enabled by this CCD ranges from 3800 to 8600 Å. At various times we used fibers with

different diameters, thus, these more recent Fairborn spectra have a resolution of either 0.24 or 0.4 Å, corresponding to resolving powers of 25,000 or 15,000 at 6000 Å. These spectra have S/Ns generally ranging from 100 to 150. The various telescope and detector combinations plus the resulting spectrum information are summarized in Table 1.

Our KPNO observations are single-order spectra of limited wavelength coverage. To reduce the effects of blends on the radial velocities, instead of cross-correlating the entire region, we measured velocities of the lines in the five least blended regions of spectra with the IRAF cross-correlation program FXCOR (Fitzpatrick 1993). We used a Gaussian to fit the cross-correlation function of the lines in the chosen regions. We employed the IAU radial-velocity standards β Vir and HR 5694 as the cross-correlation reference stars for our KPNO spectra. From Scarfe (2010) we adopt radial velocities of 4.4 and 54.4 km s^{-1} for β Vir and HR 5694, respectively. Our KPNO velocities are listed in Table 2.

The AST echelle spectra contain 21 useful orders. Rather than cross-correlating each order to obtain an average velocity and then determining which orders produce discrepant velocities, we chose to measure individual unblended lines. We used a solar-type star line list, consisting of 168 lines between 4920 and 7100 Å, and fitted Gaussians to the individual lines. Thus, unlike the KPNO velocities, those from Fairborn Observatory are on an absolute scale.

We have unpublished measurements of the radial velocities of several IAU solar-type velocity standards. After comparing those results with the velocities of Scarfe (2010) for the same stars, we added $+0.3 \text{ km s}^{-1}$ to our SITe CCD velocities and $+0.6 \text{ km s}^{-1}$ to our Fairchild CCD velocities to adjust the velocity zero points so that the KPNO and Fairborn results are on a consistent scale. The average velocities for our Fairborn spectra also are given in Table 2.

3. Spectroscopic Orbit

Initially, we obtained orbits of the 2.1241 day velocity variations of HD 126516 with the computer program BISP (Wolfe et al. 1967) and refined those elements with SB1 (Barker et al. 1967). However, those orbits showed systematic velocity residuals. We next employed the general least-squares program of Daniels (1966) to obtain a simultaneous orbital solution of the primary’s short- and long-period velocity variations. With all elements varied, we determined separate orbital solutions for the KPNO and Fairborn velocities.

With the rather short period of 2.1241 days, the close pair would be expected to have a circular orbit if it were just a binary system (Zahn 1977; Hut 1981; Duquenois & Mayor 1991). But the effects of the long-period companion in the HD 126516 system could produce a modulation of the eccentricity (e.g., Mazeh & Shaham 1979; Söderholm 1984).

Table 2
Radial Velocity Observations of HD 126516

Hel. Julian Date HJD–2,400,000	RV (km s ⁻¹)	$O - C$ (km s ⁻¹)	Phase _L ^a	RV _L (km s ⁻¹)	Phase _S ^b	RV _S (km s ⁻¹)	Observatory ^c
51738.711	7.4	-0.35	0.378	-20.88	0.094	27.93	KPNO
51742.707	12.9	-0.10	0.384	-20.70	0.975	33.50	KPNO
52015.846	-58.8	-0.06	0.772	-27.71	0.567	-31.14	KPNO
52016.910	3.3	-0.02	0.774	-27.71	0.067	30.99	KPNO
52708.910	-6.3	0.16	0.759	-27.17	0.855	21.03	KPNO
52709.954	-46.7	0.08	0.760	-27.29	0.347	-19.33	KPNO
52755.859	4.3	0.35	0.825	-28.56	0.958	33.21	KPNO
52756.733	-51.8	0.39	0.827	-28.54	0.370	-22.86	KPNO
52757.725	-11.2	0.12	0.828	-28.85	0.837	17.77	KPNO
52757.893	0.3	-0.11	0.828	-29.08	0.916	29.27	KPNO
52758.742	-42.5	0.13	0.829	-28.87	0.316	-13.50	KPNO
52758.904	-55.6	-0.13	0.830	-29.13	0.392	-26.59	KPNO
52759.740	-21.4	0.11	0.831	-28.92	0.785	7.63	KPNO
52759.906	-6.9	-0.14	0.831	-29.18	0.864	22.14	KPNO
53119.842	-34.3	-0.01	0.343	-20.12	0.318	-14.19	KPNO
53171.736	-21.4	-0.27	0.417	-21.33	0.750	-0.35	KPNO
53173.764	-31.5	-0.80	0.420	-21.89	0.704	-10.41	KPNO
53350.044	-36.9	-0.10	0.671	-25.48	0.696	-11.51	Fair
53356.023	-60.0	-0.49	0.679	-26.05	0.510	-34.43	Fair
53387.006	1.0	-0.38	0.724	-26.90	0.097	27.53	Fair
53400.035	-22.9	-0.03	0.742	-26.98	0.231	4.05	Fair
53410.036	4.3	0.01	0.756	-27.27	0.939	31.58	Fair
53422.915	6.6	0.30	0.775	-27.41	0.003	34.31	Fair
53427.000	2.6	0.07	0.780	-27.78	0.926	30.45	Fair
53427.988	-53.8	0.42	0.782	-27.47	0.391	-25.92	Fair
53440.951	-62.4	-0.08	0.800	-28.41	0.494	-34.08	Fair
53455.946	-61.1	-0.15	0.822	-28.97	0.553	-32.28	Fair
53469.901	-5.0	-0.06	0.842	-29.33	0.123	24.27	Fair
53482.781	-17.0	-0.49	0.860	-30.12	0.187	12.64	Fair
53492.839	0.2	0.05	0.874	-29.83	0.922	30.08	KPNO

Notes.^a The subscript L refers to the long-period orbit.^b The subscript S refers to the short-period orbit.^c KPNO = Kitt Peak National Observatory, Fair = Fairborn Observatory.

(This table is available in its entirety in machine-readable form.)

The short-period eccentricity determined from the Fairborn velocities is quite small, 0.0030 ± 0.0009 , and its longitude of periastron is $260^\circ \pm 17^\circ$. The value from the KPNO solution is also small, 0.005 ± 0.001 , and that solution has a longitude of periastron of $306^\circ \pm 12^\circ$. Thus, the eccentricities and orbital orientations of the two solutions are similar. The precepts of Lucy & Sweeney (1971) indicate that the small value of the eccentricity for the short-period orbit should be retained. However, the eccentricity found from both solutions is so small that random errors may well dominate the results, and so we have chosen to adopt a circular orbit for the short-period pair.

The period of the outer orbit is 702.7 days or 1.92 yr, and its eccentricity is moderate with a value of 0.36. Thus, the period ratio of the long- to short-period orbit is 331.

The center-of-mass velocities of the KPNO and Fairborn solutions differ by just 0.1 km s^{-1} . In addition, the variances of the two solutions are similar, indicating that the individual velocities should be given nearly equal weights in a combined solution. Thus, for our final solution we combined the data sets, assigned unit weights to all velocities, and assumed that the short-period orbit is circular.

The resulting orbital elements and related quantities are listed in Table 3. In that table, parameter symbols with

subscript S are for the short-period system, and parameter symbols with subscript L are for the long-period system. Also in that table, the short-period orbital element T_0 is a time of maximum radial velocity, which occurs at 0.25 phase units before primary eclipse. For each observation the individual velocity of the primary star and its residual to the combined fit of the short- and long-period velocity variations are given in Table 2. Also listed in that table are the short- and long-period fractional phases. In addition, for plotting purposes the calculated short-period radial velocity plus the total velocity residual and the calculated long-period radial velocity plus the total velocity residual are tabulated. Those radial velocities are compared with the short- and long-period velocity curves in Figures 1 and 2, respectively. The short-period set of velocities will also be used to obtain the combined photometric-spectroscopic solution.

4. Photometric Observations and Reductions

We acquired our photometric observations of HD 126516 on 236 nights during its 2002–2003 and 2006–2007 observing seasons with the Tennessee State University T3 0.4 m Automatic Photoelectric Telescope (APT) at Fairborn. The

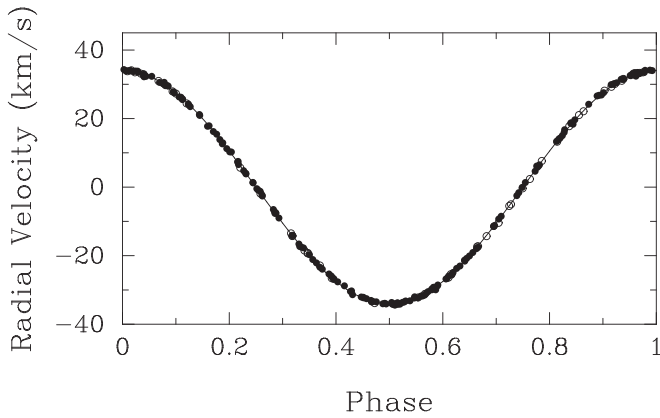


Figure 1. The 2.1241 day radial-velocity curve of the primary of HD 126516 in the short-period orbit. Each point represents the observed velocity minus its center-of-mass velocity in the long-period orbit, calculated from the elements in Table 3. Open circles = KPNO, solid circles = Fairborn Observatory. The solid line is the calculated velocity curve. Zero phase is a time of maximum velocity.

Table 3

HD 126516 Spectroscopic Orbital Elements and Related Parameters

Parameter	Value
P_L (days)	702.71 ± 0.25
T_L (HJD)	$2,454,986.68 \pm 1.39$
e_L	0.3565 ± 0.0046
ω_L (deg)	244.21 ± 0.98
K_L (km s^{-1})	5.523 ± 0.029
γ (km s^{-1})	-23.828 ± 0.020
$a_L \sin i$ (10^6 km)	49.86 ± 0.28
$f(m)_L$ (M_\odot)	0.01000 ± 0.00017
P_S (days)	$2.12408284 \pm 0.00000037$
T_0^a (HJD)	$2,454,939.50467 \pm 0.00029$
e_S	0.0 (adopted)
K_S (km s^{-1})	34.019 ± 0.024
$a_S \sin i$ (10^6 km)	0.99363 ± 0.00067
$f(m)_S$ (M_\odot)	0.008665 ± 0.000018
Standard error of an observation of unit weight (km s^{-1})	0.3

Note.

^a A time of maximum radial velocity.

precision photometer of T3 uses an EMI 9924B photomultiplier tube (PMT) that measures photon count rates successively through Johnson *B* and *V* filters. To maximize the precision of the observations, the PMT, voltage divider, pre-amplifier electronics, and all photometric filters are mounted within the temperature- and humidity-controlled body of the photometer. The telescope was programmed to make differential observations with respect to both a comparison star (HD 124115, $V = 6.42$, $B - V = 0.48$, F7V) and a check star (HD 123739, $V = 6.80$, $B - V = 1.02$, K0). The typical precision of a single observation on good nights was usually in the range of ~ 0.0025 – 0.0035 mag, as measured from the scatter in the check minus comparison star differential magnitudes. Further details on the telescope and photometer, observing techniques, and data reduction procedures can be found in Henry (1995a, 1995b) and Eaton et al. (2003).

On most nights (228), we programmed the APT to make several observations of HD 126516 at intervals of an hour or so to define the out-of-eclipse light curve of the system. On the

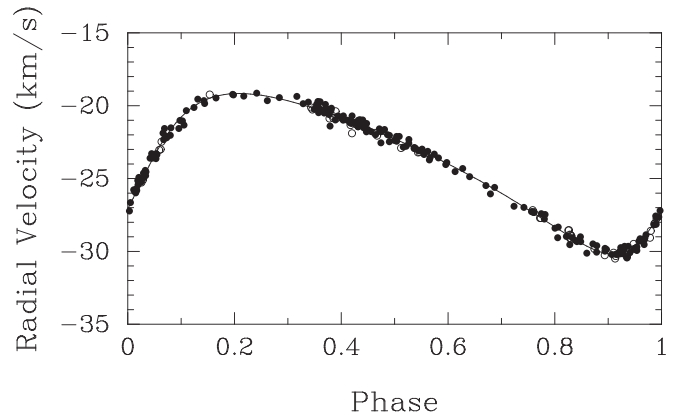


Figure 2. The 702.7 day long-period orbit of the primary of HD 126516. Each point represents the observed velocity minus its velocity in the short-period orbit that was calculated from the elements in Table 3. Open circles = KPNO velocities, solid circles = Fairborn Observatory velocities. Solid line is the calculated velocity curve. Zero phase is a time of periastron passage.

Table 4

Photometric Observations of HD 126516^a

HJD–2,400,000.0	Phase ^b	ΔV	ΔB
52635.0308	0.8234	1.868	1.825
52640.0167	0.1708	1.870	1.829
52641.0154	0.6409	1.876	1.828
52643.0083	0.5792	1.877	1.834
52645.0031	0.5183	1.875	1.839
52646.0014	0.9883	1.922	1.876
52648.9909	0.3957	1.880	1.834
52649.9909	0.8665	1.864	1.833
52650.9883	0.3361	1.877	1.835
52651.9828	0.8043	99.999	1.834
52652.9807	0.2741	1.869	1.834
52653.9798	0.7445	1.866	1.834
52654.9750	0.2130	1.866	1.828
52655.9733	0.6830	1.868	1.839
52656.9704	0.1524	1.871	99.999
52657.9701	0.6231	1.872	99.999

Notes.

^a 99.999 signifies that the differential magnitude was discarded because its internal standard deviation exceeded 0.01 mag.

^b The fractional phases are based on parameter values listed in Table 7.

(This table is available in its entirety in machine-readable form.)

remaining eight nights, we acquired higher-cadence monitoring observations to cover the primary eclipse. All observations are given in Table 4. Specific details of the nightly and the monitoring observations can be found in Fekel et al. (2013a), which describes identical observations of the star VV Crv.

5. Combined Light and Velocity Solution

Although the short-period binary components eclipse and we have obtained both spectroscopic and photometric observations of the system, significant information to enable a well-determined combined solution is missing. While we have obtained an excellent short-period spectroscopic orbit, the lines of the secondary are not visible, so the mass ratio cannot be determined from our spectra. In addition, the system has a modest primary eclipse depth and the large temperature difference of the components produces a nearly nonexistent secondary eclipse. Nevertheless, a Wilson-Devinney (WD)

Table 5
Measurement Characteristics

Curve	Data Points	Normal Mag	σ^a
Johnson <i>V</i>	624	1.8696	0.0052
Johnson <i>B</i>	652	1.8278	0.0035
RV ₁	234	...	0.31 km s ⁻¹

Note.^a For the light curves, in units of total light at phase 0.25.**Table 6**
Nonvarying WD Parameters

Parameter	Symbol ^a	Value
Albedo (bol)	A_1, A_2	0.500, 0.500
Gravity darkening	g_1, g_2	0.300, 0.300
Limb darkening (bol)	x_1, y_1	+0.116, +0.603
Limb darkening (bol)	x_2, y_2	-0.165, +0.726
Limb darkening (<i>V</i>)	x_1, y_1	+0.115, +0.687
Limb darkening (<i>V</i>)	x_2, y_2	+0.039, +0.906
Limb darkening (<i>B</i>)	x_1, y_1	+0.303, +0.580
Limb darkening (<i>B</i>)	x_2, y_2	+0.118, +0.853

Note.^a Subscripts 1 and 2 denote the more massive and less massive components, respectively, of the short-period binary.

analysis of our combined data can help to define the system's basic parameters. However, they may have significantly larger uncertainties than usual.

For our combined light and velocity solutions we used the 2013 version of the WD program. The physical model of that program is described in detail in Wilson & Devinney (1971), Wilson (1979, 1990, 2012a, 2012b), Van Hamme & Wilson (2007), and Wilson et al. (2010). Different sections of the WD program are used depending on the configuration of the system. Given the main-sequence spectral type of the primary and that estimated for the secondary, as discussed below, for HD 126516 we used mode 2, which is for detached systems. All observations in each data set were assigned unit weight. Our curve-dependent weights were computed from the standard deviations listed in Table 5. Light-level dependent weights were applied inversely proportional to the square root of the light level. Gravity darkening, g , and bolometric albedo, A , coefficients for both components were fixed at the canonical convective-envelope values from Lucy (1967). We adopted a square-root limb-darkening law with coefficients x, y from Van Hamme (1993) for both components, and we used the detailed reflection treatment of Wilson (1990) with two reflections. Table 6 contains the values of our nonvarying parameters.

To estimate the effective temperature, T_{eff} , of the primary, we examined the spectral type and photometry of HD 126516. Moore & Paddock (1950) gave a spectral type of F3 V, while Houk & Swift (1999) classified HD 126516 as F2/3 V in the Michigan Spectral Survey. More recently, Fekel et al. (2003) found a slightly later type of F5 IV-V that is nearly identical to the F5 V spectral type of Kahraman Alicavus et al. (2016). From the Tycho observations (Hog et al. 2000) we used $V = 8.306$ mag and $B - V = 0.434$. Additionally, Olsen obtained a $b - y$ value of 0.287 (Olsen 1983) and an $H\beta$ value of 2.667 (Olsen & Perry 1984). The results for $B - V$,

$b - y$, and $H\beta$ all point to a spectral type of F5 V for the primary. No lines of the short-period secondary are seen in our spectra nor are lines of the tertiary visible. Given the agreement of $B - V$, $b - y$, and $H\beta$, we started with F5 V type characteristics. From Flower (1996), the $B - V$ corresponds to $T_{\text{eff}} = 6568$ K, so we chose 6600 K as the initial estimate of the primary's temperature. This is in agreement with the effective temperatures of 6590 ± 120 K and 6800 ± 200 K found respectively by Bruntt et al. (2008) and Kahraman Alicavus et al. (2016) from their abundance analyses. From the mass function of the short-period orbit (Table 3), a canonical mass of $1.35 M_{\odot}$ for the F5 V star (e.g., Gray 1992; Cox 2000; Eker et al. 2018), and an inclination of 90° because the system is eclipsing, we estimate the mass of the short-period secondary to be about $0.29 M_{\odot}$. This suggests the secondary is a mid-M dwarf, which would have $B - V \sim 1.6$ and a T_{eff} around 3100 K (Eker et al. 2018).

For our joint photometric-spectroscopic solution, we used the short-period velocities listed in Table 2 that were determined from the combined solution of both spectroscopic orbits. Each of those velocities consists of its calculated short-period radial velocity plus its total velocity residual.

We adopted the orbital elements from our initial spectroscopic solution along with the temperatures mentioned above as starting values for our combined WD solutions. With radial velocities from only one component, the mass ratio of the secondary to the primary, $q = M_2/M_1$, could not be determined from the spectroscopic observations. Thus, similar to Zhang et al. (2015) and Wang et al. (2019), we obtained WD solutions for a range of mass ratios in steps of 0.002. The adopted value was the one for which the sum of the squared residuals of the eclipse light-curve solution was smallest. The solution values produced a broad minimum, so, as suggested by the referee, we adopted a 5% change for the uncertainty of the mass ratio resulting in a mass ratio of 0.212 ± 0.012 . For an inclination of 85° , this mass ratio range of 0.200–0.224 corresponds to a mass range for the primary of 1.57 – $1.16 M_{\odot}$, respectively. For the secondary, the range of q values gives a mass range of 0.31 – $0.26 M_{\odot}$. Holding the mass ratio constant at the value of 0.212, we then produced WD runs on all of the data and adjusted the inclination, semimajor axis, both surface potentials, temperature of the secondary, radial velocity of the center of mass, period, epoch, and light normalization parameters. We assumed both components rotated synchronously and used the solar metal abundances. Initial solutions produced no evidence of light from the third component, so the third-light parameter was not further utilized. After the best solution was found, we adjusted the primary's temperature in steps of 100 K and redetermined the solution using all of the variable parameters; however, none of these needed additional refinement. The sums of the squares of the residuals for these solutions were almost identical, but the smallest corresponded to a 6500 K temperature for the primary. From this technique we estimate its uncertainty as 200 K. The period of the short-period orbit for this 6500 K solution is identical within its uncertainty to the value from the spectroscopic solution alone. Thus, we next obtained a joint photometric-spectroscopic solution with the period fixed at the spectroscopic value.

With the effective temperature of the secondary as a variable, the WD program found a best solution temperature of 3950 K for that component. However, because the relative depths of the two eclipses determine the temperature ratio, the extremely

Table 7
Light and Velocity Curve Results for HD 126516^a

Parameter	Symbol ^b	Value
Period (days)	P	2.12408284 ^c
Epoch of primary eclipse minimum (HJD)	T_0	$2,454,940.03580 \pm 0.00025$
Eccentricity	e	0.0 ^c
Systemic velocity (km s^{-1})	γ	-0.008 ± 0.023
Semimajor axis (R_\odot)	a	8.182 ± 0.008
Inclination (deg)	i	85.8 ± 0.3
Mass ratio	M_2/M_1	0.212 ^c
Surface potential	Ω_1	5.15 ± 0.03
Surface potential	Ω_2	7.13 ± 0.05
Effective temperature (K)	T_1	6500 ^c
Effective temperature (K)	T_2	3100 ^c
Luminosity ratio	$L_1/(L_1 + L_2)_V$	0.9997 ± 0.0002
Luminosity ratio	$L_1/(L_1 + L_2)_B$	0.9999 ± 0.0002

Notes.

^a WD simultaneous solution, including proximity and eclipse effects, of the light and velocity data.

^b Subscripts 1 and 2 denote the more massive and less massive components, respectively, of the short-period binary.

^c Adopted value, see Sections 3 and 5 in the text.

shallow depth of the secondary eclipse in HD 126516 results in a very large secondary temperature uncertainty, and the value of 3950 K is quite inconsistent with the WD solution secondary mass and radius values. From an extensive analysis of over 500 eclipsing binary components, Eker et al. (2018) obtained mass–luminosity, mass–radius, and mass–temperature relations for main-sequence stars with masses between $0.18 M_\odot$ and $31 M_\odot$. Comparing our results with the empirical mass, radius, and temperature results of Eker et al. (2018), we have chosen to fix the effective temperature of the secondary at 3100 K. This new WD solution, with the temperature of the secondary fixed but the other parameters either fixed or varied as discussed previously, is our final one. From the two different temperatures of the secondary, we estimate an uncertainty of 900 K. However, we note that adopting the much lower temperature for the secondary has no significant effect on the properties of the primary, which are our main interest in obtaining the eclipse solution.

The orbital elements for this solution of a detached system are given in Table 7. Figure 3 plots our V and B observations compared with their respective light-curve solutions. Below those two curves are the V and B residuals from the fitted curves.

While the values in Table 7 are the results from our best solution with the WD software, the uncertainties from that solution of some of the quantities will be underestimated. As noted previously, because of the large mass ratio of the short-period binary components, the secondary lines are not visible; therefore, the mass ratio cannot be determined from our spectra. In addition, the primary has a very modest primary eclipse depth of just 0.05 mag in Johnson V , and the large temperature difference of the components results in a nearly nonexistent secondary eclipse (see Figure 3). This has caused us to fix not just the temperature of the primary, as is typically done in WD solutions, but also the mass ratio and temperature of the secondary.

To establish more realistic uncertainties, we performed a Monte Carlo analysis using the technique described by Lester et al. (2019).

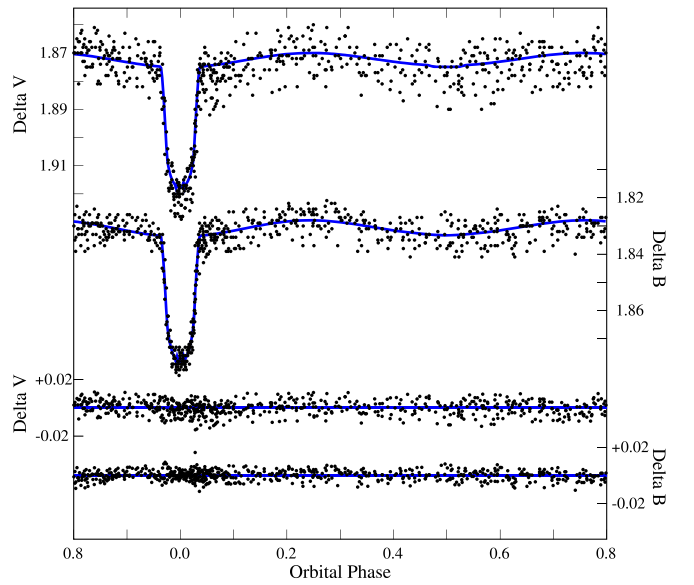


Figure 3. Top two phase plots show the differential Johnson V and B magnitudes of HD 126516 = V349 Vir fitted with the WD light curves. Zero phase is mid primary eclipse. The lower two plots are the V and B residuals from the fitted curves. The horizontal lines correspond to a residual of zero.

Again, the mass ratio was varied in steps of 0.002 from 0.200 to 0.224. We randomly varied each observational data point, both the time and the magnitude or radial velocity, in a uniform distribution based on the standard deviation computed for each data set by the WD program. Then we re-ran the best WD solution for that particular mass ratio. The randomization and the WD analyses were performed 200 times per mass ratio. In each case, we ran a simultaneous solution of the three data sets. In Table 7 the uncertainties come from the Monte Carlo analysis.

The WD program computes geometrical sizes of the two stars. Relative radii are given in four directions: from the center toward the poles, toward the sides, toward the back, and toward the point. The WD program also calculates an equal-volume, mean radius, $\langle r \rangle$, for each star and the percentage of the Roche lobe, $\langle r \rangle / \langle r \rangle_{\text{lobe}}$, that is filled, being 39% and 15% for the primary and secondary, respectively. The relative radii are listed in Table 8, and Figure 4 is an image of the system at phase 0.25 to demonstrate the relative shapes and orbital separation.

From our best joint photometric-spectroscopic solution, the resulting masses are $M_1 = 1.34 \pm 0.20 M_\odot$ and $M_2 = 0.28 \pm 0.03 M_\odot$, and the equal-volume radii are $R_1 = 1.66 \pm 0.08 R_\odot$ and $R_2 = 0.30 \pm 0.02 R_\odot$ for the primary and secondary, respectively. In Table 9 these values are listed as well as other fundamental parameters of the components. The mass and radius uncertainties have been estimated from the range of the mass ratio value while the other parameter uncertainties are from the Monte Carlo simulations. In the case of the adopted temperature values, their uncertainties were discussed in Section 5.

6. Discussion

As noted earlier, Moore & Paddock (1950) classified HD 126516 as F3 V, while Houk & Swift (1999) gave it a spectral type of F2/3 V. These classifications are slightly earlier than those of Fekel et al. (2003), who found F5 IV-V,

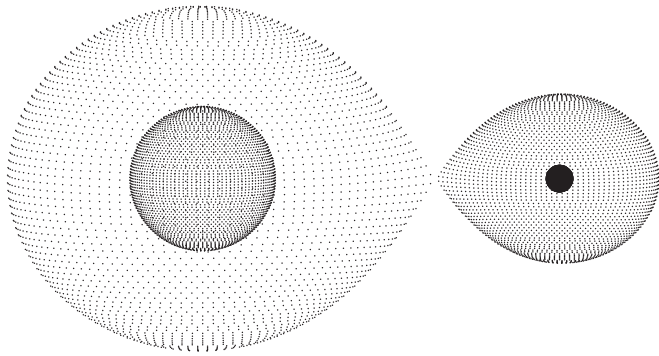


Figure 4. Image of the eclipsing components of HD 126516 at phase 0.25. The filled Roche lobes are indicated by overlaying the resulting WD plot from the Mode 6 (contact binary) option for our solution.

Table 8
Model Relative Radii^a for HD 126516

Parameter	Value
r_1 (pole)	0.2023 ± 0.0012
r_1 (point)	0.2040 ± 0.0012
r_1 (side)	0.2033 ± 0.0012
r_1 (back)	0.2038 ± 0.0012
$\langle r_1 \rangle^b$	0.2032 ± 0.0013
$\langle r_1 \rangle / \langle r_1 \rangle_{\text{lobe}}$	0.3920 ± 0.0024
r_2 (pole)	0.0369 ± 0.0003
r_2 (point)	0.0369 ± 0.0003
r_2 (side)	0.0369 ± 0.0003
r_2 (back)	0.0369 ± 0.0003
$\langle r_2 \rangle^b$	0.0365 ± 0.0003
$\langle r_2 \rangle / \langle r_2 \rangle_{\text{lobe}}$	0.1452 ± 0.0001

Notes.

^a Subscripts 1 and 2 denote the more massive and less massive components, respectively, of the short-period binary.

^b Equal-volume mean radii.

Table 9
Fundamental Parameters of HD 126516

Parameter	Primary	Secondary
$M(M_{\odot})$	1.34 ± 0.20	0.28 ± 0.03
$R(R_{\odot})$	1.66 ± 0.08	0.30 ± 0.02
L/L_{\odot}	4.42 ± 0.55	0.008 ± 0.002
M_{bol} (mag)	3.13 ± 0.13	10.1 ± 0.28
$\log g$ (cm s^{-2})	4.13 ± 0.01	4.93 ± 0.01
T (K)	6500^a	3100^a

Note.

^a Adopted value, see Section 5 in the text.

and Kahraman Alicavus et al. (2016), who determined F5 V. From Tycho the $B - V$ color of HD 126516 is 0.434 (Hog et al. 2000), and it has an $H\beta$ value of 2.667 (Olsen & Perry 1984), both of which are consistent with an F5 V spectral type.

We searched our photometric data sets minus the eclipse points for evidence of γ Dor frequencies in the range $0.01\text{--}30.0 \text{ day}^{-1}$, corresponding to 0.033–100 days, following the methods described by Henry et al. (2011). No evidence

for γ Dor frequencies was found in our light curves of HD 126516. This result plus the lack of line profile variations (De Cat et al. 2006) and mid-F spectral class of HD 126516 causes us to conclude that HD 126516 is not a γ Dor pulsator.

From their spectroscopic analyses of HD 126516, Bruntt et al. (2008) determined an effective temperature of $6590 \pm 120 \text{ K}$ and a $\log g = 4.01 \pm 0.15$, while Kahraman Alicavus et al. (2016) obtained a similar effective temperature of $6800 \pm 200 \text{ K}$ and a $\log g = 4.2 \pm 0.2$. These values overlap our values of an effective temperature of $6500 \text{ K} \pm 200 \text{ K}$ and $\log g = 4.13 \pm 0.01$.

Using an effective temperature of 6590 K, Bruntt et al. (2008) determined a metallicity relative to the Sun, $[M/H]$, of -0.19 ± 0.08 , which was computed as the average of the elements Ca, Sc, Ti, Cr, and Fe. Their value of the Fe abundance, $[Fe/H]$, is -0.23 , and thus is similar to the above metallicity. Kahraman Alicavus et al. (2016) determined a slightly higher effective temperature of 6800 K from their iron abundance analysis. Converting the logarithm of their number abundance relative to hydrogen, 7.50, into a logarithmic value relative to the Sun (Albrecht et al. 2009) results in $[Fe/H] = 0.0$. Thus, the iron abundance of the two analyses are close to or equal to the solar value.

A comparison of our best-fit properties for the $1.34 M_{\odot}$ primary with the stellar evolutionary tracks from the Yonsei–Yale series (Yi et al. 2001; Demarque et al. 2004) produces $[Fe/H] = -0.14$, a value between the spectroscopically determined values of Bruntt et al. (2008) and Kahraman Alicavus et al. (2016), and results in an age of $2.5 \pm 1.0 \text{ Gyr}$. Casagrande et al. (2011) reanalyzed the basic properties of over 15,000 solar-type solar neighborhood stars in the Geneva–Copenhagen Survey. For HD 126516 they determined a likely age of 2.4 Gyr, which is in good agreement with our result.

The parallax, ϖ , values of $10.881 \pm 0.069 \text{ mas}$ from *Gaia*/DR2 (*Gaia* Collaboration et al. 2018) and $9.14 \pm 1.24 \text{ mas}$ from *Hipparcos* (van Leeuwen 2007) both result from the adoption of a single star model. With the offset value of Stassun & Torres (2018) the *Gaia* parallax becomes slightly larger, 10.963 mas. Comparing the corrected *Gaia* and *Hipparcos* values, there is a 20% difference between the two, and while the *Gaia* parallax has a much smaller uncertainty and so might be preferred, at present the *Gaia* results for bright stars still have some calibration issues that have not been completely resolved (D. Pourbaix 2018, private communication). For comparison, our basic parameters result in a parallax of $9.22 \pm 0.55 \text{ mas}$, a value similar to that of van Leeuwen (2007).

With its V magnitude of 8.306 mag (Hog et al. 2000) and the revised *Gaia*/DR2 parallax of $10.963 \pm 0.076 \text{ mas}$ (*Gaia* Collaboration et al. 2018; Stassun & Torres 2018) the primary of HD 126516 has an absolute visual magnitude, M_V , of 3.51 ± 0.02 . Assuming the $B - V$ color from Tycho (Hog et al. 2000), we adopted an effective temperature and bolometric correction from Table 3 of Flower (1996). We then used the Stefan–Boltzmann law to determine additional properties. From spectral-type and temperature calibration uncertainties, we estimate an effective temperature uncertainty of $\pm 200 \text{ K}$. The resulting luminosity for HD 126516 is $3.06 \pm 0.07 L_{\odot}$ and its radius is $1.35 \pm 0.08 R_{\odot}$. If the *Hipparcos* parallax of van Leeuwen (2007) is used instead, M_V is increased to $3.1 \pm 0.3 \text{ mag}$, the luminosity becomes $4.4 \pm 1.2 L_{\odot}$, and the radius is increased to $1.6 \pm 0.2 R_{\odot}$.

Table 10
Comparison of Fundamental Parameters of HD 126516

Parameter	Eclipse	<i>Hipparcos</i> Parallax Solution	<i>Gaia</i> Parallax Solution ^a
	Solution	(van Leeuwen 2007)	(<i>Gaia</i> Collaboration et al. 2018)
ϖ (mas)	9.22 ± 0.55	9.14 ± 1.24	10.963 ± 0.076
T_{eff} (K)	6500 ± 200	6568 ± 200	6568 ± 200
M_{bol} (mag)	3.13 ± 0.13	3.1 ± 0.3	3.52 ± 0.02
L (L_{\odot})	4.42 ± 0.55	4.4 ± 1.2	3.06 ± 0.07
R (R_{\odot})	1.66 ± 0.08	1.6 ± 0.2	1.35 ± 0.08

Note.

^a The systematic offset of Stassun & Torres (2018) is included.

Table 10 compares these results with those from our best combined light and velocity solution. The values from the revised *Hipparcos* parallax of van Leeuwen (2007) are in good agreement with our combined solution, while the more precise values from the *Gaia* parallax (*Gaia* Collaboration et al. 2018), which includes the modest systematic offset of Stassun & Torres (2018), are in poorer agreement.

From our best solution, the combined mass of the 2.1241 day system is $1.62 M_{\odot}$. Like the secondary of the short-period system, no lines of the tertiary are seen in our spectra. Thus, it is significantly fainter, likely at least 2.5 mag (Stockton & Fekel 1992), than the primary of the system. From this information and value of the mass function of the long-period system, which is $0.010 M_{\odot}$ (Table 3), the tertiary has a mass that ranges from 0.34 to about $0.8 M_{\odot}$ and an orbital inclination that ranges from 90° to 25° . Thus, assuming that the third component is a single main-sequence star, it is a K or M dwarf.

HD 126516 is a hierarchical triple system consisting of a short-period binary and third component with a much longer orbital period. The long-period to short-period ratio for the system is 331. If the inclination difference between the inner and outer orbits of such a system is large enough, then the eccentricity and inclination of the short-period orbit can undergo periodic changes, which are known as Kozai–Lidov cycles (Kozai 1962; Lidov 1962). Various theoretical analyses have concluded that the evolution of such triple systems is driven by the Kozai–Lidov modulation plus tidal friction, which results in the inner binary having a period of just a few days (Mazeh & Shaham 1979; Eggleton & Kiseleva-Eggleton 2001; Fabrycky & Tremaine 2007). In particular, Fabrycky & Tremaine (2007) have predicted that the combination of Kozai–Lidov cycles and tidal friction usually produces inner binaries with periods less than 10 days with the peak of their final short-period distribution being 3 days. Observationally, Tokovinin et al. (2006) examined a sample of 165 solar-type binaries and found that 96% of those with periods less than 3 days were triple. With its inner binary having a period of 2.1241 days, HD 126516 clearly is consistent with the results of Fabrycky & Tremaine (2007) and Tokovinin et al. (2006).

Zahn (1977) and Tassoul & Tassoul (1992) have explored different mechanisms for orbital circularization and rotational synchronization. While their analyses produced very different absolute timescales for circularization and synchronization, the two mechanisms predict that synchronization should occur first. As shown in Section 3, the 2.1241 day orbit of HD 126516 is circular and thus we would expect that the rotational velocity of the primary is synchronized with the

orbital period. Adopting our radius of $1.66 R_{\odot}$ and assuming that the orbital and rotational inclinations are the same, we find that the rotational velocity of the primary is 40 km s^{-1} . However, the primary of the short-period eclipsing binary has very narrow lines. Fekel et al. (2003) determined a $v \sin i$ value of $4.1 \pm 1.0 \text{ km s}^{-1}$, while De Cat et al. (2006) measured $3.8 \pm 0.3 \text{ km s}^{-1}$, and Kahraman Alicavus et al. (2016) found $5 \pm 1 \text{ km s}^{-1}$. Averaging the three results produces a mean of 4.3 km s^{-1} . With an orbital inclination of 86° from Table 7 and the orbital and rotational axes aligned, then this $v \sin i$ value would be the rotational velocity. But, if the primary is indeed synchronously rotating, then the inclination of its rotational axis must be extremely small, just 6.2° . Thus, either the rotation of the primary is not synchronized with the orbital period, which would be surprising because the star is not young but has a moderate age of 2.5 Gyr and its orbit is circularized, or there is a very large spin–orbit misalignment.

Close binaries are generally expected to have their rotational and orbital axes aligned because they were born together in the same part of a molecular cloud, but there are situations, such as the presence of a third companion, that could produce misalignment after birth (Anderson et al. 2017). Observationally, there have only been about three dozen systems that have been examined for rotational-axis alignment of the components with their orbital axes, and the majority of these systems are short-period mass-transfer eclipsing binaries (see Albrecht et al. 2011, 2014). Over the course of the past decade or so, the most extensive analyses have been done by Albrecht and collaborators, who have observed several young, detached, early-type binaries and measured the changes in the line profile of the eclipsed star, the Rossiter–McLaughlin effect (McLaughlin 1924; Rossiter 1924), to determine the alignment of the axes. They found at least two very young binaries, DI Her (age 4.5 Myr) and CV Vel (age 40 Myr), that have spin–orbit misalignments (Albrecht et al. 2009, 2014). Both systems are relatively massive having early-B components and also have very eccentric orbits. On the other hand, for NY Cep, which has early-type B-star components and orbital parameters that are very similar to DI Her, they found close spin–orbit alignment (Albrecht et al. 2011). Likewise, the components of the mid-B type system EP Cru are also aligned (Albrecht et al. 2013). In a significantly less massive system, V1143 Cyg, which consists of two F5 V components, Albrecht et al. (2007) again found spin–orbit alignment. Thus, misaligned rotation axes have been confirmed, but so far in only two very young systems (Albrecht et al. 2011).

For HD 126516 the $v \sin i$ value of 4 km s^{-1} for the short-period primary of the eclipsing system is clearly at odds with the expected value of 40 km s^{-1} that is computed for synchronous rotation. The apparent axial misalignment of the F5 V primary of HD 126516 might be the result of dynamical interactions with the third component of the system. However, the theoretical analysis of Hut (1981) indicates that the timescales for orbital circularization and spin–orbit axial alignment are similar. More recently, Anderson et al. (2017, p. 3067) stated that “If tidal dissipation is sufficiently strong to circularize the orbit, it will almost certainly align the spin axis with the orbital axis on a shorter timescale.” Thus, the reason for the strikingly different values of the observed and expected rotational velocity of the primary of HD 126516 remains uncertain.

While a useful astrometric solution for the 702.7 day orbit is not feasible with the *Hipparcos* data, the more precise results from *Gaia* may allow such an orbit to be computed enabling the long-period orbital inclination to be determined. Such a result will improve our knowledge of the mass of the third star and permit a comparison of the short- and long-period orbital inclinations to determine whether the orbits might be coplanar.

We thank Walter Van Hamme (Florida International University) for helpful instructions and discussions about the WD program's various procedures. We also thank D. Barlow, who computed a very preliminary short-period orbit. The anonymous referee provided useful suggestions that improved this paper. We appreciate informative conversations with Kurt Wiesenfeld (Georgia Tech) regarding Monte Carlo simulations and error bar formulas. Astronomy at Tennessee State University is supported by the state of Tennessee through its Centers of Excellence program. Our research made use of the SIMBAD database, operated by CDS in Strasbourg, France. This work also made use of data from the European Space Agency (ESA) mission *Gaia* (<https://www.cosmos.esa.int/gaia>), processed by the *Gaia* Data Processing and Analysis Consortium (DPAC; <https://www.cosmos.esa.int/web/gaia/dpac/consortium>). Funding for the DPAC has been provided by national institutions, in particular the institutions participating in the *Gaia* Multilateral Agreement.

ORCID iDs

Francis C. Fekel  <https://orcid.org/0000-0002-9413-3896>
 Gregory W. Henry  <https://orcid.org/0000-0003-4155-8513>

References

- Albrecht, S., Reffert, S., Snellen, I., Qirrenbach, A., & Mitchell, D. S. 2007, *A&A*, **474**, 565
- Albrecht, S., Reffert, S., Snellen, I. A. G., & Winn, J. N. 2009, *Natur*, **461**, 373
- Albrecht, S., Setiawan, J., Torres, G., Fabrycky, D. C., & Winn, J. N. 2013, *ApJ*, **767**, 32
- Albrecht, S., Winn, J. N., Carter, J. A., Snellen, I. A. G., & de Mooij, E. J. W. 2011, *ApJ*, **726**, 68
- Albrecht, S., Winn, J. N., Torres, G., et al. 2014, *ApJ*, **785**, 83
- Anderson, K. R., Lai, D., & Storch, N. I. 2017, *MNRAS*, **467**, 3066
- Asplund, M., Grevesse, N., Sauval, A. J., & Scott, P. 2009, *ARA&A*, **47**, 481
- Barker, E. S., Evans, D. S., & Laing, J. D. 1967, *RGOB*, **130**, 355
- Bruntt, H., De Cat, P., & Aerts, C. 2008, *A&A*, **478**, 487
- Casagrande, L., Schönrich, R., Asplund, R., et al. 2011, *A&A*, **530**, A138
- Cox, A. N. 2000, *Allen's Astrophysical Quantities* (4th ed.; New York: Springer)
- Daniels, W. 1966, Univ. of Maryland, Dept. of Physics and Astronomy Tech. Rep. No. 579
- De Cat, P., Eyer, L., Cuypers, J., et al. 2006, *A&A*, **449**, 281
- Demarque, P., Woo, J.-H., Kim, Y.-C., & Yi, S. K. 2004, *ApJS*, **155**, 667
- Duquenois, A., & Mayor, M. 1991, *A&A*, **248**, 485
- Eaton, J. A., Henry, G. W., & Fekel, F. C. 2003, in *Astrophysics and Space Science Library*, Vol. 288, *The Future of Small Telescopes in the New Millennium: Volume II—The Telescope We Use*, ed. T. D. Oswalt (Dordrecht: Kluwer), 189
- Eaton, J. A., & Williamson, M. H. 2004, *Proc. SPIE*, **5496**, 710
- Eaton, J. A., & Williamson, M. H. 2007, *PASP*, **119**, 886
- Eggleton, P. P., & Kiseleva-Eggleton, L. 2001, *ApJ*, **562**, 1012
- Eker, Z., Bakis, V., Bilir, S., et al. 2018, *MNRAS*, **479**, 5491
- Fabrycky, D., & Tremaine, S. 2007, *ApJ*, **669**, 1298
- Fekel, F. C., Henry, G. W., & Sowell, J. R. 2013a, *AJ*, **146**, 146
- Fekel, F. C., Rajabi, S., Muterspaugh, M. W., & Williamson, M. H. 2013b, *AJ*, **145**, 111
- Fekel, F. C., Warner, P., & Kaye, A. B. 2003, *AJ*, **125**, 2196
- Fitzpatrick, M. J. 1993, in *ASP Conf. Ser. 52, Astronomical Data Analysis Software and Systems II*, ed. R. J. Hanisch, R. V. J. Brissenden, & J. Barnes (San Francisco, CA: ASP), 472
- Flower, P. J. 1996, *ApJ*, **469**, 355
- Gaia* Collaboration, Brown, A. G. A., Vallenari, A., et al. 2018, *A&A*, **616**, A1
- Gray, D. F. 1992, *The Observation and Analysis of Stellar Photospheres* (Cambridge: Cambridge Univ. Press), 431
- Handler, G. 1999, *MNRAS*, **309**, L19
- Henry, G. W. 1995a, in *ASP Conf. Ser. 79, Robotic Telescopes: Current Capabilities, Present Developments, and Future Prospects for Automated Astronomy*, ed. G. W. Henry & J. A. Eaton (San Francisco, CA: ASP), 37
- Henry, G. W. 1995b, in *ASP Conf. Ser. 79, Robotic Telescopes: Current Capabilities, Present Developments, and Future Prospects for Automated Astronomy*, ed. G. W. Henry & J. A. Eaton (San Francisco, CA: ASP), 44
- Henry, G. W., Fekel, F. C., & Henry, S. M. 2011, *AJ*, **142**, 39
- Hog, E., Fabricius, C., Makarov, V. V., et al. 2000, *A&A*, **355**, L27
- Houk, N., & Swift, C. 1999, *Michigan Catalogue of Two-Dimensional Spectral Types for the HD Stars*, Vol. 5 (Ann Arbor, MI: Univ. Michigan Press)
- Hut, P. 1981, *A&A*, **99**, 126
- Kahraman Alicavus, F., Niemczura, E., De Cat, P., et al. 2016, *MNRAS*, **458**, 2307
- Kaye, A. B., Handler, G., Krisciunas, K., Poretti, E., & Zerbi, F. M. 1999, *PASP*, **111**, 840
- Kazarovets, E. V., Samus, N. N., Durlevich, O. V., Kireeva, N. N., & Pastukhova, E. N. 2008, *IBVS*, **5863**, 1
- Kozai, Y. 1962, *AJ*, **67**, 591
- Lester, K. V., Gies, D. R., Schaefer, G. H., et al. 2019, *AJ*, **157**, 140
- Lidov, M. L. 1962, *P&SS*, **9**, 719
- Lucy, C. B., & Sweeney, M. A. 1971, *AJ*, **76**, 544
- Lucy, L. B. 1967, *ZA*, **65**, 89
- Mazeh, T., & Shoham, J. 1979, *A&A*, **77**, 145
- McLaughlin, D. B. 1924, *ApJ*, **60**, 22
- Moore, J. H., & Paddock, G. F. 1950, *ApJ*, **112**, 84
- Olsen, E. H. 1983, *A&AS*, **54**, 55
- Olsen, E. H., & Perry, C. L. 1984, *A&AS*, **56**, 229
- Otero, S. A., & Wils, P. 2005, *IBVS*, **5630**, 1
- Perryman, M. A. C. & ESA 1997, *The Hipparcos and Tycho Catalogues* (Noordwijk: ESA)
- Pojmanski, G. 2002, *AcA*, **52**, 397
- Rossiter, R. A. 1924, *ApJ*, **60**, 15
- Scarfe, C. D. 2010, *Obs*, **130**, 214
- Söderhelm, S. 1984, *A&A*, **141**, 232
- Stassun, K. G., & Torres, G. 2018, *ApJ*, **862**, 61
- Stockton, R. A., & Fekel, F. C. 1992, *MNRAS*, **256**, 575
- Tassoul, J.-L., & Tassoul, M. 1992, *ApJ*, **395**, 259
- Tody, D. 1986, *Proc. SPIE*, **627**, 733
- Tody, D. 1993, in *ASP Conf. Ser. 52, Astronomical Data Analysis Software and Systems II*, ed. R. H. Hanisch, R. J. V. Brissenden, & J. Barnes (San Francisco, CA: ASP), 173
- Tokovinin, A. 2008, *MNRAS*, **389**, 925
- Tokovinin, A., Thomas, S., Sterzik, M., & Udry, S. 2006, *A&A*, **450**, 681
- Van Hamme, W. 1993, *AJ*, **106**, 2096
- Van Hamme, W., & Wilson, R. E. 2007, *ApJ*, **661**, 1129
- van Leeuwen, F. 2007, *Hipparcos, The New Reduction of the Raw Data* (Berlin: Springer)
- Wang, K., Zhang, X., Luo, Y., & Luo, C. 2019, *MNRAS*, **486**, 2462
- Wilson, R. E. 1979, *ApJ*, **234**, 1054
- Wilson, R. E. 1990, *ApJ*, **356**, 613
- Wilson, R. E. 2012a, *JASS*, **29**, 115
- Wilson, R. E. 2012b, *AJ*, **144**, 73
- Wilson, R. E., & Devinney, E. J. 1971, *ApJ*, **166**, 605
- Wilson, R. E., Van Hamme, W., & Terrell, D. 2010, *ApJ*, **723**, 1469
- Wolfe, R. H., Horak, H. G., & Storer, N. W. 1967, in *Modern Astrophysics*, ed. M. Hack (New York: Gordon and Breach), 251
- Yi, S. K., Demarque, P., Kim, Y.-C., et al. 2001, *ApJS*, **136**, 417
- Zahn, J.-P. 1977, *A&A*, **57**, 383
- Zhang, X. B., Luo, Y. P., & Wang, K. 2015, *AJ*, **149**, 96